

PreScope: Unleashing the Power of Prefetching for Resource-Constrained MoE Inference

Enda Yu, Zhaoning Zhang*, Dezun DONG*, Yongwei Wu, Xiangke Liao
 {yuenda,zhangzhaoning,dong,xkliao}@nudt.edu.cn,wuyw@tsinghua.edu.cn
 National University of Defense Technology, Tsinghua University
 China

Abstract

Mixture-of-Experts (MoE) models reduce inference computation via sparse activation, yet encounter a dual bottleneck, memory constraints and PCIe latency, when deployed on commodity hardware: deploying a 10B parameter MoE on a single commodity GPU, for example, requires offloading expert weights to CPU memory, and the resulting on-demand PCIe transfer latency often exceeds that of the associated GPU computation by several folds. Hybrid CPU-GPU co-execution is a promising remedy, but faces three intertwined challenges: 1) inaccurate prediction of expert activation patterns, rendering prefetching ineffective; 2) competition for limited PCIe bandwidth between expert prefetching and on-demand loading; and 3) high complexity in cross-device scheduling. We present PreScope, a prediction-driven dynamic expert scheduling system that addresses these challenges with three co-designed contributions. First, we discover that expert activations exhibit distinct group-wise patterns across layers—near-input, near-output, and middle layers each show unique characteristics. Accordingly, we propose the Learnable Layer-Aware Predictor (LLaPor), a module explicitly designed to achieve high-precision expert selection prediction by distinguishing and leveraging these layer-group-specific traits. Second, we propose the Prefetch-Aware Cross-Layer Scheduling strategy (PreSched), a strategy that quantifies global performance gains, across all MoE layers, rather than confining to local optimality within individual layers, while intelligently balancing the trade-offs between prefetching costs and on-demand loading overhead, and generates globally optimal scheduling plans. Third, we design an Asynchronous I/O Optimizer (AsyncIO) that decouples I/O operations from computation, overlaps PCIe transfers with GPU/CPU kernel execution, and effectively eliminates idle waiting bubbles. PreScope achieves end-to-end inference throughput improvements of 141% over the state-of-the-art solutions, and decoding latency reductions of 74.6%, providing an efficient solution for MoE deployment in resource-constrained environments.

Keywords: Mixture-of-Experts; Offloading; LLM Inference

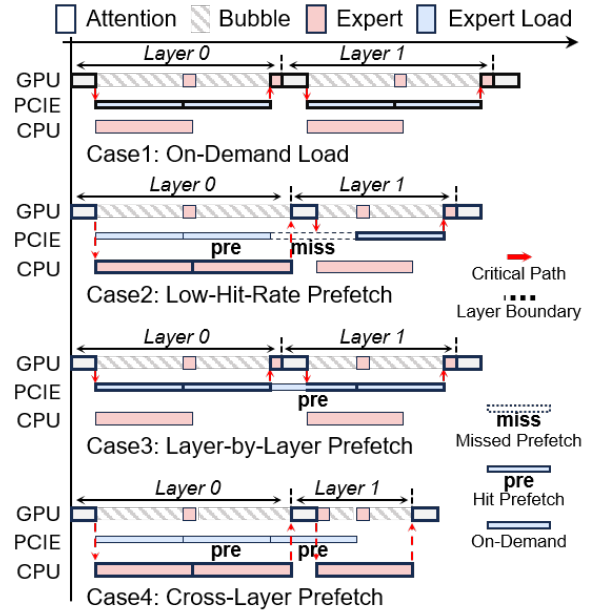


Figure 1. Impact of prefetching on inference latency.

1 Introduction

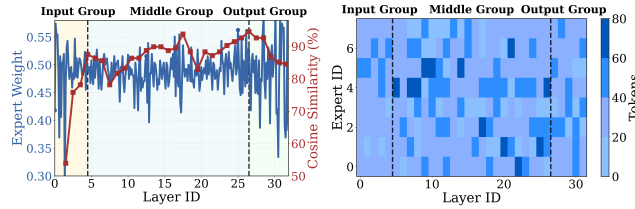
Mixture of Experts (MoE) [20, 27, 29, 43] models enhance computational efficiency in large language models via sparse activation, yet face a critical memory bottleneck in resource-constrained environments [21, 23, 34]. For example, loading all experts of Mixtral-8x7B [20] requires 80GB memory, far exceeding the 32GB capacity of NVIDIA V100 GPU.

Expert offloading [5, 53, 54, 57] is the primary approach to mitigating memory bottlenecks: experts are kept in CPU memory or SSD [11, 33, 35] and loaded into GPU on demand. This inevitably introduces I/O overhead that exceeds GPU computation time and leaves idle gaps between adjacent layers. To fill these gaps, expert-prefetching strategies [10, 11, 56, 57] have been widely studied. Fate [10] predicts routing by exploiting similarity in adjacent-layer gating inputs, yet it cannot eliminate the fundamental mismatch between compute duration and I/O latency. Klotski [11] increases batch size to cover I/O latency, but it also increases the total number of activated experts. Fiddler [22] and kTransformers [4] allow CPU execution of experts missing GPU cache, but lack precise scheduling for hot experts

*Zhaoning Zhang, Dezun Dong is the Corresponding Author

Table 1. Comparison of MoE offloading systems.

Work	Expert Computation	Prefetch Strategy	Scheduling Strategy	Load Balancing
Fate [10]	GPU	Gate	CPU-blind	✗
Klotski [11]	GPU	Expert	CPU-blind	☆
Fiddler [22]	CPU+GPU	None	Prefetch-blind	☆
HybriMoE [57]	CPU+GPU	Gate	Prefetch-blind	★
ours	CPU+GPU	Expert-Gate	Prefetch-aware	★★

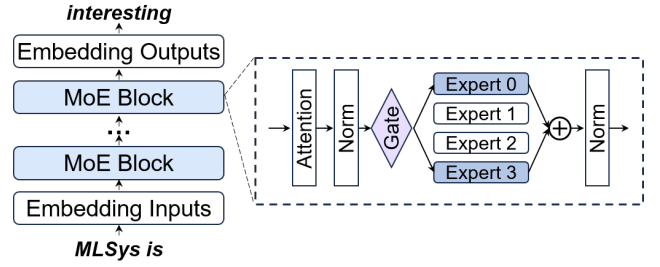
**Figure 2.** Group-wise characteristics of expert weight, inter-layer cosine similarity, and activation distribution in MoE.

(experts processing more tokens), resulting in high CPU overhead (up to 67% per layer). HybriMoE [57] introduces a queuing mechanism to prioritize hot experts on GPU, yet its greedy placement strategy optimizes only per-layer latency, overlooking cross-layer optimization enabled by prefetching. A comparative analysis is provided in Table 1.

While CPU–GPU co-execution offers a promising direction, existing solutions struggle with three fundamental challenges: **Prediction Uncertainty**. Expert activation varies sharply across layers. Traditional prediction methods based on statistics or gating inputs fail to track these shifts (Figure 6), causing mispredictions that waste PCIe bandwidth (Case2 in Figure 1). **PCIe Resource Competition**. Prefetch and on-demand loads share limited bandwidth, and the layer-by-layer execution model always prioritizes the latter. Without coordination, when conflicts arise, prefetch degrades to on-demand loading of the next layer. **Cross-Device Scheduling Complexity**. CPUs and GPUs differ dramatically in throughput and latency, forcing prior work to schedule each expert greedily as soon as a thread is free. The inability to model prefetch gains and losses results in suboptimal performance.

In response to these challenges, this paper proposes PreScope, a prediction-driven cross-layer expert scheduling system. The core findings and contributions are as follows:

1. Layer-group properties. Earlier work observed inter-layer routing correlation [51], cosine similarity of gating inputs [10, 57], and hot-expert emergence [6, 18, 22]. We show that these properties obey *layer-group* structure: MoE networks naturally decompose into **input**, **output**, and **middle** groups. As shown by Mixtral-8×7B in Figure 2, input and output groups exhibit stronger routing correlation and more skewed gating weights, whereas middle layers show higher cosine similarity and dominant hot experts.

**Figure 3.** Architecture and inference process of MoE models.

2. Cross-layer prefetch efficiency. Figure 1 (Case 3 vs. 4) shows that the layer-by-layer scheduling loads two experts to GPU to accelerate next layer startup, and repeats this at Layer 1, resulting in more I/O. Cross-layer scheduling instead uses one of the I/O slots to prefetch Layer 1 experts, slightly increasing Layer 0 latency yet reducing total latency. Passive, local prefetching inflates CPU idle time; globally, it fails to pipeline GPU, I/O, and CPU. Prefetch must therefore be managed proactively inside a global cost model.

3. Predictability of inference overhead. CPU time grows linearly with token count, while PCIe and GPU times are largely token-invariant. By acquiring the token distribution of the current and prefetch-target layers, we can estimate cross-layer latency via pipeline modelling.

Based on these insights, PreScope introduces three co-designed innovations:

- **LLaPor**: a layer-aware lightweight predictor that uses distinct architectures for each layer group, exploits both inter-layer routing correlation and adjacent-layer cosine similarity statistics, achieves a Top-4 prediction accuracy of over 90%, with support for online continuous learning.
- **PreSched**: a prefetch-aware cross-layer scheduler that builds a unified cost model to dynamically optimize expert placement by quantifying the global benefits of prefetching and on-demand loading, thereby breaking through the limitations of greedy strategies.
- **AsyncIO**: an asynchronous I/O optimizer that decouples expert movement from computation, pipelines transfers across heterogeneous memories, and splits each expert into fine-grained chunks to saturate PCIe bandwidth.

Extensive evaluation on Mixtral-8×7B [20], DeepSeek-MoE [27], Qwen3 [43], and Moonlight [29] shows that PreScope boosts end-to-end inference throughput by 141% over Klotski and 70.8% over HybriMoE, while cutting decoding latency by 74.6% and 42.1%, respectively, providing an efficient solution for MoE deployment in resource-constrained environments.

2 Background and Related Work

2.1 Inference of MoE Models

MoE is one of the dominant architectures for large language models [20, 27, 32]. As illustrated in Figure 3, the model

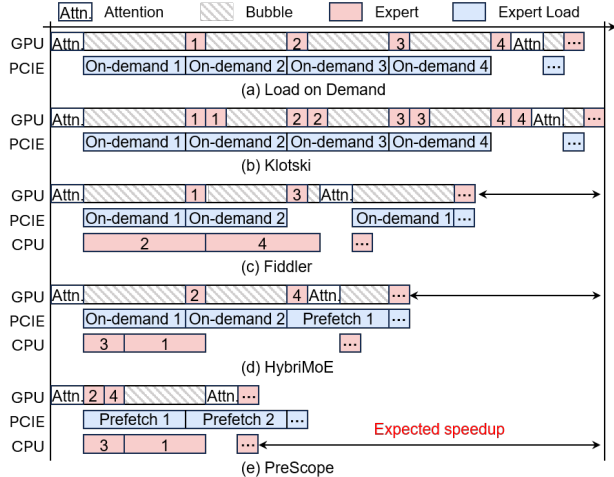


Figure 4. Execution timeline comparison of various methods. We reduce the pipeline bubble through accurate prefetching and cross layer scheduling.

consists of multiple stacked MoE blocks. For an input token x , the processing within one MoE block can be summarized as follows: the hidden state a is computed by the attention layer and fed into a gating network, which uses a softmax to compute routing weights and selects the top- k most relevant experts. Their outputs are aggregated via a weighted sum to produce the block output x' , which is then passed to the next block. This process can be expressed with the following equations:

$$\begin{aligned}
 a &= \text{Attention}(x) \\
 \text{top}[0 \dots k], \quad w_i &= \text{Gate}(a) \\
 x' &= \sum_{i=0}^{k-1} w_i \cdot \text{Expert}_i(a)
 \end{aligned} \tag{1}$$

A key observation is that once the hidden state a and current gating output are fixed, the expert activation pattern in subsequent layers becomes deterministic, since the parameters of all functional modules remain unchanged. This determinism provides a theoretical foundation for the design of LLaPor.

2.2 MoE Offloading

MoE models face severe memory bottlenecks during inference; offloading [37, 40, 41, 47] is an effective remedy. MoE-Lighting [3] keeps the KV-cache in host memory and performs attention on the CPU. PowerInfer [39] places neurons on the GPU or CPU according to their activation frequency. Tabi [44] partitions the model into segments and executes only a subset on the GPU while running the remainder on the CPU. Our work targets the expert-placement problem, which is the main source of performance bottlenecks in the inference process of MoE models.

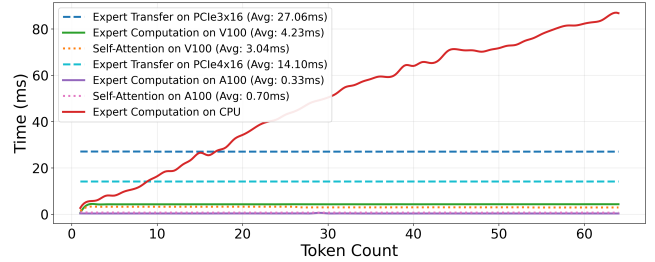


Figure 5. Characterization of expert computation and transfer costs across heterogeneous devices.

On-demand loading methods, such as Lina [26] and ExpertFlow [16], exclusively utilize GPUs for expert computation. If an expert is not prefetched to the GPU, it must be loaded on demand, as shown in Figure 4. The downside of these approaches is the high I/O overhead, which causes prolonged GPU idling. MoE-GEN [48] mitigates this by deferring expert loading until the number of tokens targeting that expert reaches a preset threshold. Likewise, Klotski [11] enlarges the batch size to amortize the cost of loaded experts, thereby masking I/O overhead to some extent. To further reduce the I/O bubble, Fiddler [22] and kTransformers [4] propose hybrid CPU-GPU inference to lower the frequency of on-demand expert loading. They allow expert computations on the CPU and then transfer the results to the GPU. This body of work has inspired many subsequent studies and has theoretical validity. HybriMoE [57] introduces a queue that re-orders experts by token count, dispatching hot experts to the GPU and cold ones to the CPU. It uses a greedy algorithm to minimize per-layer computation cost and prefetches experts for the next layer during non-expert computations to further reduce on-demand loading pressure. PreScope retains HybriMoE’s queue but enriches the scheduler with cross-layer prefetch gains and their associated I/O costs, avoiding the sub-optimal local decisions of pure greedy policies.

2.3 CPU-GPU Collaborative Inference

Improving cooperative-inference efficiency [7, 45, 55] is a system-level challenge that embraces model compression [9, 13, 31, 42], activating fewer experts [14, 15, 30, 54], and kernel-level optimizations [17, 23, 36].

Our goal is orthogonal: we optimize without sacrificing accuracy and remain agnostic to both the model and the inference framework. Figure 5 quantifies the token-count dependence of compute and I/O cost for Mixtral-8×7B. Because the CPU’s parallel throughput is limited, its per-expert compute cost grows almost linearly with the number of tokens, whereas GPU compute and PCIe-transfer costs stay flat. With optimizations such as pinned host memory and asynchronous transfers, we achieved 79% PCIe bandwidth utilization. Under these conditions, transferring two experts

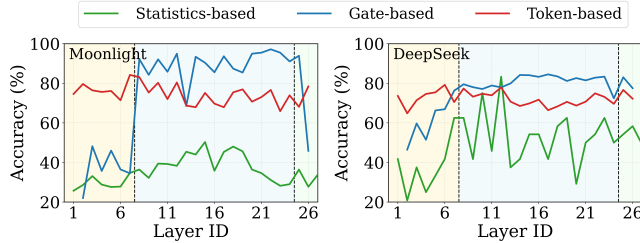


Figure 6. Comparison of three existing expert activation prediction strategies.

concurrently costs no less than transferring them serially, so expert traffic can be modelled as a sequential process. This observation forms the basis of our inference-cost model.

2.4 MoE Prefetching

In MoE inference, prefetching hot experts for subsequent layers increases I/O-computation overlap [10, 52, 57]. Prior methods exploit distinct activation patterns: Klotski [11] and MoE-Infinity [50] rely on the gating network’s bias toward hot experts; ExFlow [51] detects inter-layer routing correlations; Fate [10], InfiniGen [25] and HybriMoE [57] use the cosine similarity of gating inputs to predict expert activation. Another line of research adopts learned predictors for higher accuracy: ExpertFlow [16] and OpenMoE [49] match token-level similarity to forecast activations, whereas SiDA [8] applies embedding-based hashing and exceeds 90% hit rate on Switch-Base-128 [12]. Pre-Gated MoE [19] and ProMoE [38] explicitly model cross-layer correlations between gating inputs and expert activations, yielding high-accuracy predictors with negligible training overhead.

However, analysis across Mixtral [20], DeepSeek [27], Moonlight [29], and Qwen3 [43] shows that these properties exhibit pronounced layer-group dependence rather than uniform behaviour. A single heuristic therefore gives only limited accuracy within specific layer groups; effective prediction requires combining multiple features tailored to the target group. We elaborate in Section 3.1.

3 Motivation

3.1 Observation of Expert Layer Groups

As a case study in Figure 2, Mixtral-8x7B illustrates the correlation between expert routing weights, input cosine similarity, expert distribution, and layer groups. The same pattern holds for the other models (detailed results omitted due to space constraints). Building on Equation 1, we further analyze: in input and output layer groups, certain expert weights w_i dominate the output aggregation, amplifying the correlation of expert routing across layers. Hence, predictors should weigh previous-layer activations and their routing weights more heavily. In middle layer groups, balanced expert weights lead to the gating inputs a highly similar across

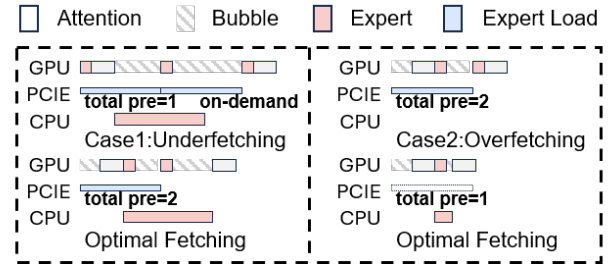


Figure 7. Two suboptimal prefetching scenarios caused by layer-by-layer scheduling.

layers, and the router tends to select hot experts. Thus, predictors here should focus more on the gating input a from the preceding layer.

3.2 Limitations of Existing Prediction Methods

Figure 6 compares the expert prediction accuracy of three strategies during inference decoding in DeepSeek and Moonlight. The statistics-based method is only effective in middle layer groups by leveraging hot expert distributions. The gate-based strategy, which utilizes high cosine similarity of gating inputs across adjacent layers, performs especially well in middle layer groups, with slightly lower accuracy in input and output groups. The token-based approach employs a light predictor to model token-expert and expert-expert correlations, achieving better performance in input and output layer groups. These comparisons highlight that leveraging expert activation properties must be layer-group-aware. Manually identifying or statistically capturing these properties per group remains challenging. In contrast, using relevant variables as input features for a neural predictor to learn these associations in a data-driven manner offers a more feasible solution.

3.3 Limitations of Layer-by-Layer Scheduling

The mainstream approach to expert placement in CPU-GPU cooperative inference uses a greedy, layer-by-layer scheduler that balances CPU cost T_C and GPU cost T_G to minimize the current layer’s completion time. This is formulated as:

$$\arg \min_{E_{cpu}, E_{gpu}} \max(T_C, T_G) \quad (2)$$

When on-demand loading coexists with prefetching, however, we observe two systematic inefficiencies. First, if the previous layer is GPU-bound ($T_G > T_C$), its on-demand loads preempt prefetch bandwidth for the target layer, forcing additional on-demand loads later and raising end-to-end latency (Figure 7, Case 1). Second, if the previous layer is CPU-bound ($T_C > T_G$), the scheduler greedily fills the PCIe pipe by prefetching experts that should be on the CPU, delaying the target layer’s compute start and again increasing latency (Figure 7, Case 2).

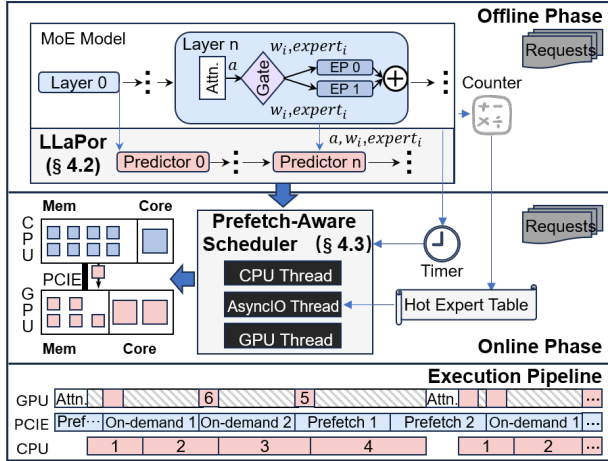


Figure 8. System overview of PreScope.

The root cause is that layer-wise schedulers optimise only the current layer’s cost, ignoring the activation pattern of the prefetch-target layer. This results in uncertain prefetching decisions—whether and how many experts to prefetch. Therefore, incorporating the expert activation status of both the current and target layers into the scheduling decision space can enable more efficient prefetch scheduling in terms of timing and frequency.

4 PreScope Design

4.1 Overview

We introduce PreScope, a prediction-driven inference system that tackles the memory-wall and PCIe-latency-wall faced by MoE inference in resource-constrained environments. Figure 8 shows the system overview of PreScope.

In the offline phase we profile the target model over multiple iterations to build the dataset for training the Learnable Layer-Aware lightweight Predictor (LLaPor). The Timer records per-operation costs, while the Counter ranks experts by the number of processed tokens to produce a hot-expert table. Given the available GPU memory, the system loads the hottest experts in descending order until the memory budget is exhausted. During online inference the Timer continuously monitors the execution pipeline, while LLaPor predicts expert activations for upcoming layers from the current-layer inputs. The Prefetch-aware Cross-layer Scheduler (PreSched) combines Timer feedback with LLaPor forecasts to make real-time decisions that minimize pipeline bubbles. The Asynchronous I/O Optimiser (AsyncIO) decouples expert movement from computation, transfers experts asynchronously across heterogeneous memories, and splits each transfer into fine-grained chunks to maximize PCIe throughput. LLaPor continually ingests new runtime data to adapt to evolving task patterns.

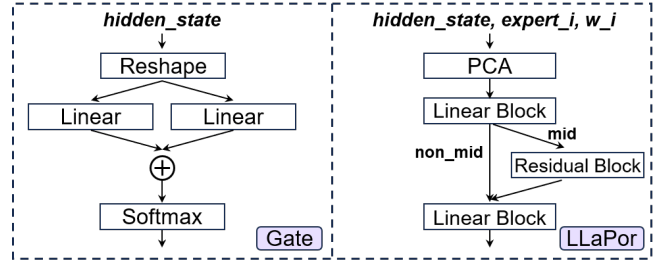


Figure 9. Architectural comparison between the standard gating network and LLaPor.

4.2 Learnable Layer-aware Predictor

4.2.1 Network Architecture of LLaPor. Building on the analysis in Section 2.1, we collect the hidden state a , the indices of the activated experts $expert_i$, and their corresponding weights w_i per layer as feature variables during the offline phase. At training time, we use the previous-layer features to predict expert activations in the current layer.

LLaPor is inspired by the native MoE gating network but builds an independent lightweight predictor for every MoE block. As shown in Figure 9, LLaPor first compresses the hidden state a with Principal Component Analysis (PCA) to cut training cost, then fuses the reduced features. Instead of the single linear transform used in the gating network, each linear block in LLaPor consists of a linear layer, GELU activation, and Dropout for more robust feature learning.

Reflecting the layer-group differentiation in MoE models, predictors assigned to the input and output groups use shallow networks to avoid over-fitting on the noisier features typical of these layers. Predictors for the middle groups are deeper and contain an additional residual block composed of stacked linear layers, GELU activations and dropout; a gating unit modulates this block to capture the influence of the hidden state a on expert activation.

4.2.2 Training Strategy of LLaPor. LLaPor employs a layer-group-differentiated training strategy, with variations in the loss function, feature variables, and optimizer.

Loss Function Predictors in input and output groups are trained using a hybrid loss function designed to address class imbalance and improve learning on hard samples. The overall loss combines an expert-balancing loss L_{expert} and a focal loss term L_{focal} , expressed as $L = L_{\text{expert}} + \lambda \cdot L_{\text{focal}}$, where λ is a weighting hyperparameter. The expert-balancing term incorporates inverse expert frequency $1/f_i$ to mitigate activation imbalance, and is defined as:

$$L_{\text{expert}} = -\frac{1}{N} \sum_{i=1}^N \frac{\text{BCE}(y_i, p_i)}{f_i}$$

where $y_i \in \{0, 1\}$ indicates whether expert i is activated, p_i denotes the predicted probability of expert i , N is the

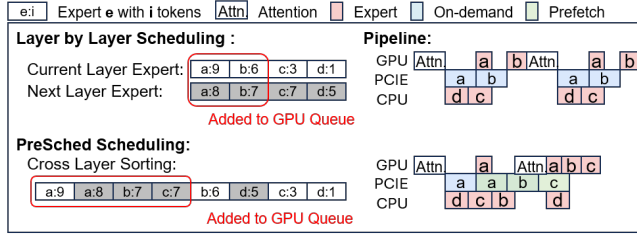


Figure 10. Comparison of PreSched scheduling versus layer-by-layer scheduling strategies.

total number of experts, and BCE refers to the binary cross-entropy loss $BCE(y_i, p_i) = y_i \log(p_i) + (1 - y_i) \log(1 - p_i)$. The focal loss term emphasizes hard misclassified examples by reducing the contribution of easy samples through a modulating factor $(1 - p_t)^\gamma$, where p_t is the predicted probability for the true label and $\gamma \geq 0$ is a focusing parameter. This term is given by:

$$L_{\text{focal}} = -\frac{1}{N} \sum_{i=1}^N (1 - p_t)^\gamma \cdot BCE(y_i, p_i)$$

Feature Variables Strong PCA compression (4096 dimensions to 256 dimensions) is applied to hidden state a in input and output groups due to high cross-layer variation; middle groups use milder compression (4096 dimensions to 512 dimensions) thanks to feature stability.

Optimizer AdamW is used with learning rates and weight decay dynamically adjusted by layer index. Input and output groups employ a composite scheduler: linear warmup for 5 epochs followed by cosine annealing for faster convergence. Middle groups use higher learning rates and weight decay to accelerate convergence and counter overfitting, leveraging their stable features and high-quality gradients. Gaussian noise and random masking are applied during training to improve generalization and robustness. LLaPor can be embedded in the inference module to collect new samples and perform online gradient updates, adapting to shifting input distributions during inference.

4.3 Prefetch-Aware Cross-Layer Scheduling

4.3.1 Design Principle. PreSched jointly optimizes expert placement for the current layer and the prefetch-target layer, maximizing the global benefit of every transfer instead of merely minimizing the current-layer latency. Traditional schedulers, confined to the current layer’s activation distribution, apply a greedy layer-wise policy. As Figure 10 illustrates, PreSched exploits LLaPor’s inter-layer predictions to expand the scheduling horizon to both layers, gaining cross-layer visibility. Under limited PCIe bandwidth it prioritizes the most heavily loaded experts, moving more tokens per transfer and shrinking PCIe idle windows. PreSched also calibrates the prefetch count so that CPU-compute bubbles

are fully exploited for loading while preventing excessive prefetch traffic from interfering with critical I/O.

4.3.2 Problem Modeling. To model the problem, the following premises and constraints are proposed:

Premise 1 (Cross-layer Sorting). The gating network provides activated experts for the current layer, and LLaPor predicts those for the next layer. After excluding experts already on the GPU or being loaded, lists $E_{\text{cur}}[0 \dots n]$ and $E_{\text{next}}[0 \dots n' - 1]$ are formed by sorting experts in ascending order of pending tokens. The two lists are then merged into $E_{\text{all}}[0 \dots n + n']$ via cross-layer ordering.

Premise 2 (On-demand Monotonicity). To maximize on-demand benefit, if $E_{\text{cur}}[i]$ requires no loading, then neither do $E_{\text{cur}}[0 \dots i - 1]$; conversely, if $E_{\text{cur}}[i]$ requires loading, so must $E_{\text{cur}}[i + 1 \dots n]$.

Constraints. Expert loading time is fixed as t_{io} ; GPU expert computation cost is t_g ; attention computation time is t_{attn} ; CPU expert cost t_c depends on token count m :

$$t_c = \beta \cdot m + C \quad (3)$$

where β is the CPU computational cost of a single token, and C is the startup cost.

Premise 3 (Prefetch Non-interruptibility). A prefetch, once started but not finished before the current layer’s computation ends, must be completed without initiating new prefetches to avoid blocking subsequent I/O.

Premise 4 (Serial I/O). All PCIe transfers have been optimized to bandwidth saturation and cannot be further parallelized, thus being regarded as a serial queue.

Premise 5 (Computation Masking). Since $t_g < t_{io}$, the GPU computation cost of any expert that has been preloaded can be completely masked by the I/O bubble and is omitted from the latency model.

The decision variable is whether $E_{\text{cur}}[i]$ needs to be loaded onto the GPU, with i recursively decremented from n to 0 until no loading is needed. The objective is to minimize the total layer latency $\Sigma_{\text{layer_latency}}$.

4.3.3 Trade-Off between On-Demand and Prefetch .

The optimal placement of experts depends on the computation location of hot experts. Based on the problem modeling constraints, the issue simplifies to choosing for expert $E_{\text{cur}}[i]$ between strategy A (on-demand load to GPU) or B (compute directly on CPU, reserving I/O bandwidth for prefetching the next layer’s experts). To quantify this trade-off, we formulate four key questions, with Figure 11 providing a visual summary of the relevant variables for clarity.

Q1: Which experts must be moved to the GPU? We establish a cross-layer cost model for $E_{\text{all}}[i]$: transfer is mandatory if the total GPU cost T_{all}^G is lower than the CPU cost T_{all}^C .

$$\begin{aligned} T_{\text{all}}^G &= \alpha + (n + n' - i + 1) \cdot t_{io} + t_g \\ T_{\text{all}}^C &= t_c(E_{\text{all}}[0 \dots i]) + t_{\text{attn}} \end{aligned} \quad (4)$$

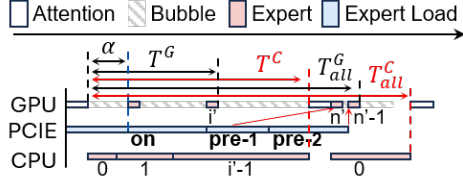


Figure 11. Mathematical modeling of PreSched balancing latency benefit.

Here, α is the delay in starting the on-demand operation due to previous prefetching, and $t_c(E_{all}[0 \dots i])$ is the total CPU computational cost of experts $E_{all}[0 \dots i]$, which can be calculated using Equation 3. If $T_{all}^G < T_{all}^C$, add $E_{all}[i \dots n+n']$ to the GPU Queue.

Since the current and predicted layers may have misaligned loads, the subsequence $E_{cur}[i' \dots n]$ belonging to the current layer in the GPU Queue is rechecked:

$$\begin{aligned} T_G &= \alpha + (n - i' + 1) \cdot t_{io} + t_g \\ T_C &= t_c(E_{cur}[0 \dots i' - 1]) \end{aligned} \quad (5)$$

If $T_G < T_C$ holds, then i' is the smallest index satisfying the condition; otherwise, the search continues inward.

Q2: Which experts will be prefetch? The gap length released by the current layer's CPU computation is:

$$T_{gap} = t_c(E_{cur}[0 \dots i' - 1]) - \alpha - (n - i' + 1) \cdot t_{io}$$

The number of prefetches $|f|$ that can be overlapped is:

$$f = \frac{T_{gap} + t_{attn}}{t_{io}} \quad (6)$$

and we round f to the nearest integer $|f|$. Experts $E_{next}[n' - |f| \dots n' - 1]$ are therefore selected for prefetching.

Q3: How to quantify prefetch gain and loss? Experts in the prefetch layer are priority-sorted, and the predictor is more accurate on hot experts; executing the highest-priority prefetch first therefore yields the largest payoff. The only prefetch that can delay an on-demand operation in the prefetch layer is the critical prefetch $|f|$. Its cost is $(|f| - f) \cdot t_e$ and its I/O benefit is $(f - |f| + 1) \cdot t_e$. Let R_{hit} and R_{miss} be the hit and miss rates of the critical prefetch. The overall benefit ξ of the critical prefetch $|f|$ is calculated as follows:

$$\xi = R_{hit} \cdot (f - |f| + 1) \cdot t_e - R_{miss} \cdot (|f| - f) \cdot t_e \quad (7)$$

If ξ is greater than 0, prefetch $|f|$ can be regarded as a less costly on-demand operation; otherwise, prefetch $|f|$ degrades to an on-demand start in the next layer.

Q4: When do prefetching yield no benefits?

When GPU Queue has no elements in E_{next} , it means that there is no GPU prefetching requirement (commonly seen in small batches). PreSched then extends the prediction window for cross-layer prefetching, following the same trade-off logic.

Algorithm 1: Prefetch-Aware Scheduling for Layer l

Initialization:

$j = 0, i = n, i' = n$ \triangleright current-layer window;
 $E_{cur}[0 \dots n], E_{next}[0 \dots n' - 1]$ \triangleright expert lists;

Event CrossLayerQueue(E_{cur}, E_{next})

$E_{all} \leftarrow \text{sort}(E_{cur} \cup E_{next})$ by token count;

for $k = 0$ to $n + n'$ do

 if $T_{all}^G(k) < T_{all}^C(k)$ then
 add $E_{all}[k]$ into GPU_Q ;

Event OnIoDone()

 OndemandLoop();
 PrefetchDecision();

Event OnCpuGpuDone()

 compute $E_{cur}[0 \dots i' - 1]$ on CPU;
 compute $E_{cur}[i' \dots n]$ on GPU;

Function OndemandLoop():

 foreach expert e in GPU_Q do

if e in E_{cur} then

$i' \leftarrow$ the index i' of e $\triangleright e = E_{cur}[i']$;
 if $T_G(i') < T_C(i')$ then
 $i \leftarrow i'$;
 break;

while $i < n + 1$ do

 load $E_{cur}[i]$;
 $i \leftarrow i + 1$ \triangleright load $E_{cur}[i' \dots n]$;

Function PrefetchDecision():

 if $GPU_Q \cap E_{next} = \emptyset$ then

 inter-layer prefetch with larger window;
 return;

 if $R_{hit}(f - |f| + 1) > R_{miss}(|f| - f)$ then

$i \leftarrow |f|$;

 else

$i \leftarrow |f| - 1$;

 while $i > 0$ do

 prefetch $E_{next}[n' - i]$;
 $i \leftarrow i - 1$ \triangleright prefetch $E_{next}[n' - i \dots n' - 1]$;

4.3.4 Algorithm Design. PreSched dynamically determines the computation location of each expert using a cross-layer cost model. The complete procedure is given in Algorithm 1. During offline profiling it collects the fixed-size variables described in Section 4.3.2 and evaluates every expert in the current layer E_{cur} as well as the predicted layer E_{next} in a single pass. First, experts requiring GPU loading are filtered and sorted in ascending token order to form the GPU queue GPU_Q . The algorithm then scans GPU_Q from the smallest-token end to identify the smallest current-layer expert index i' that satisfies $T_G < T_C$, on-demand loads the

segment $E_{cur}[i' \dots n]$ to the GPU, and immediately assigns the rest to the CPU for execution to minimize the on-demand sequence. In the next step PreSched computes the number of prefetches $|f|$ that can be overlapped with the CPU computation gap. The benefit of prefetching is quantified through hit-miss ratios. If the benefit is positive, the scheduler issues exactly $|f|$ prefetch requests, otherwise, it issues $|f| - 1$. The entire procedure is event driven. The OnIoDone event locates the experts that still need to be transferred and finalises the corresponding PCIe transactions. The OnCpuGpuDone event triggers the CPU to execute the next expert and fills the GPU compute slots, thereby forming a dual computation-I/O pipeline. The scheduler runs in $O(n)$ time and obtains prediction results in $O(1)$ time, which makes it suitable for real-time inference.

4.4 Asynchronous I/O Optimizer

To alleviate the I/O bottleneck in expert transfers within MoE models, this paper designs an asynchronous expert transmission mechanism. The core idea is to decouple computation from expert transmission, enhancing transfer efficiency through pipelined operations and increasing computation-I/O overlap, thereby significantly reducing inference latency. Specifically, the system maintains two types of pre-registered expert weight caches in GPU memory: one for on-demand loading, which uses dual buffer areas to alternate between computation waiting and expert loading for immediate requests when no prefetching occurs; the other serves as a prefetch buffer, divided into two groups handling prefetch tasks for the current and next layers, respectively. This pre-registration of cache regions eliminates the overhead of repeated memory allocation and mapping for each transfer; subsequent expert movements involve only direct writes (overwrites) within these fixed buffers, substantially reducing setup overhead. The grouped rotation design ensures that prefetching stays one layer ahead of computation, providing sufficient time for expert transfer and avoiding expert overwrite issues caused by inter-layer prefetch conflicts, thus guaranteeing computational correctness and cache validity.

At the micro level each expert is decomposed into three linear weight matrices $gate_proj$, up_proj and $down_proj$. Three independent CUDA streams are used to transfer these sub tensors concurrently. This fine-grained strategy exploits the multi-lane capability of the PCIe bus by replacing one large transfer with several sub transfers that proceed in parallel. As a result the scheduler gaps on the bus are filled so that throughput approaches the PCIe peak. In addition all transfers use pinned host memory together with asynchronous copy operations so that data movement proceeds without CPU intervention and does not block GPU computation. Compared with traditional synchronous loading or simple prefetching this mechanism achieves deep computation I/O overlap while using a fixed set of cache regions

Table 2. Configuration of evaluated MoE models.

	Mixtral	Qwen3	DeepSeek	Moonlight
Layers	32	48	26	26
Routed Experts	8	128	64	64
Activated Experts	2	8	6	6
Expert Memory (BF16)	336 MB	9 MB	16.5 MB	16.5 MB

to guarantee correctness and thereby improves both system throughput and response time.

5 Implementation

PreScope is implemented in PyTorch 2.1 [2] and the Hugging Face Transformers [46] library, comprising over 6k lines of Python code. Offline profiling involves processing 128 batches, each containing 512 tokens, while logging hidden states and expert activations per layer; these traces constitute the training dataset for LLaPor. Each layer-specific predictor is co-located with the MoE model’s forward pass, enabling direct access to architectural details. Training uses only PyTorch; the resulting checkpoints are serialized to disk and loaded at runtime via a lightweight wrapper that seamlessly integrates expert predictions during model execution.

Resident hot experts are identified offline by ranking all (layer, expert_id) pairs by empirical activation frequency. During initialization, the system queries the remaining GPU memory after accounting for non-expert parameters, buffer pools, and runtime KV Cache usage, divides this capacity by the footprint of a single expert, and loads the top-ranked experts up to the computed limit.

6 Evaluation

6.1 Experimental Setup

Platform. Evaluation is conducted on NVIDIA V100 and A100 GPUs, each providing 32 GB of memory. The V100 supports PCIe3 x16, whereas the A100 supports PCIe4 x16. The host CPU is an Intel Xeon Gold 6230R.

Models. We select four widely adopted MoE models that exhibit diverse architectural characteristics: DeepSeek-V2-Lite [27], Mixtral-8x7B [20], Qwen3-30B-A3B [43], and Moonlight-16B-A3B [29]. Table 2 summarises the key differences. Mixtral represents models with fewer but larger experts, while Qwen3, Moonlight, and DeepSeek exemplify models with more but smaller experts.

Baselines. PreScope is compared with four representative MoE inference frameworks: Fate [10] (GPU-based and highly accurate in prefetching), Fiddler [22] (static CPU-GPU hybrid inference with hot-expert preloading), Klotski [11] (reduces expert transfers by processing multiple batches in parallel), and HybriMoE [57] (CPU-GPU hybrid inference with greedy scheduling). Klotski limits itself to two-batch parallelism to avoid memory overflow. For a fair comparison, all baselines adopt our optimised expert-transfer method and the

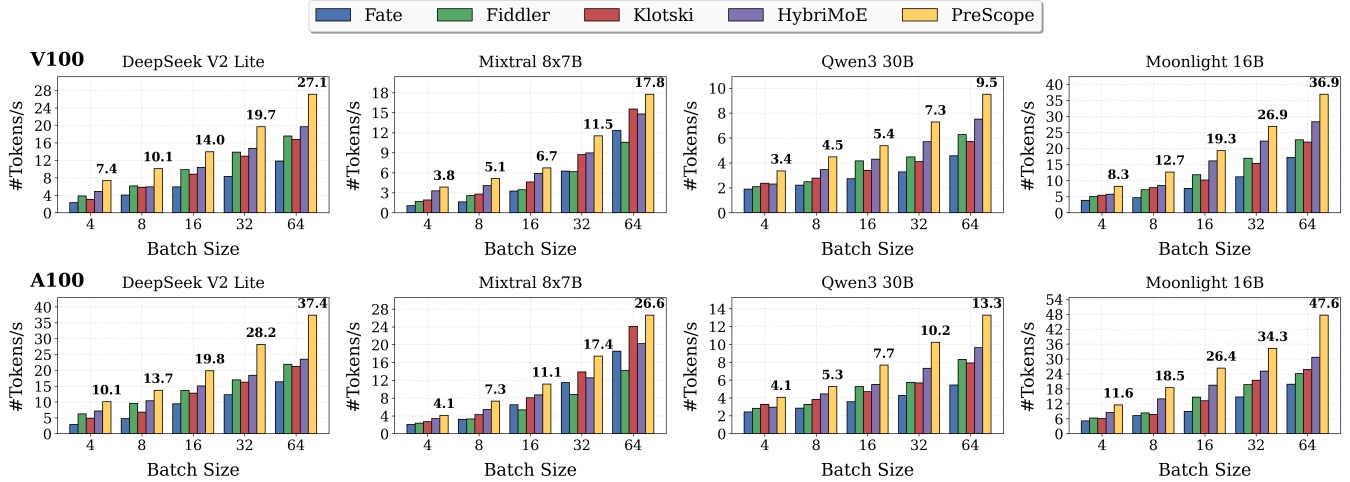


Figure 12. Throughput comparison between PreScope and baseline systems across models and hardware.

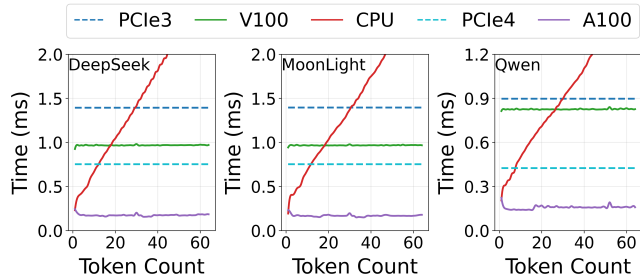


Figure 13. Characterization of expert computation and transfer costs across models and heterogeneous devices.

same hot-expert table at initialisation, but their parameter-compression mechanisms remain disabled.

Metrics. We measure throughput (tokens generated per unit of generation time) and decoding latency (time per output token). Generation time covers both the prefill and the decoding stages.

Dataset. Experiments use the ShareGPT dataset [1] with batch sizes ranging from 4 to 64, an input length of 512 tokens, and an output length of 64 tokens. To verify the generalisation capability of LLaPor, we additionally evaluate it on the DPO [24] and LLaVA [28] datasets.

6.2 End-to-End Performance

6.2.1 Overhead Characterization. Figure 13 depicts the absolute time costs of expert computation and PCIe transfer as a function of token count under different hardware configurations, revealing three key observations that quantitatively ground subsequent performance analysis. First, for both V100 and A100 GPUs, the execution time of a single expert on GPU is significantly lower than the PCIe transfer time, indicating that the performance ceiling of a GPU-only solution is I/O-bound rather than compute-bound. Second,

for the "small experts" architecture, when the number of tokens per expert is below 16, the linear computation delay on CPU is actually lower than the GPU startup delay (over 20% gap in the case of Qwen). However, as expert size increases, such as Mixtral in Figure 6, the CPU delay consistently exceeds that of GPU, demonstrating that the architecture scale directly determines the break-even point for CPU offloading. Third, as the total token count increases, the parallel computing advantage of GPU becomes prominent, while the computational overhead on CPU grows linearly, suggesting that GPU should dominate computation tasks in high-frequency or large-data-volume scenarios, otherwise the CPU may become a system bottleneck.

6.2.2 Throughput. Figure 12 illustrates the end-to-end throughput of four models on V100 and A100 GPUs versus batch size. PreScope consistently outperforms all baselines across configurations. Two scenarios are observed:

Small-Expert Models. These models contain numerous small experts per layer, making I/O latency the dominant bottleneck. GPU-only baselines such as Fate and Klotski exhibit significantly lower throughput due to frequent expert transfer overhead. When the batch size exceeds 8, Klotski’s multi-batch pipeline fails to achieve throughput scaling proportional to batch size, primarily because of the increased number of activated experts. On V100 with a batch size of 64, PreScope achieves throughput improvements of 61.4%, 66.2%, and 67.6% over Klotski, and 129%, 108%, and 114% over Fate on DeepSeek, Qwen, and Moonlight, respectively. This advantage stems from PreScope’s ability to intelligently offload part of the computation to the CPU, avoiding redundant expert transfers and thereby yielding significantly higher throughput. On A100 with a batch size of 64, PreScope achieves throughputs of 37.4, 13.3, and 47.6 tokens/s on DeepSeek, Qwen, and Moonlight, respectively. Compared to

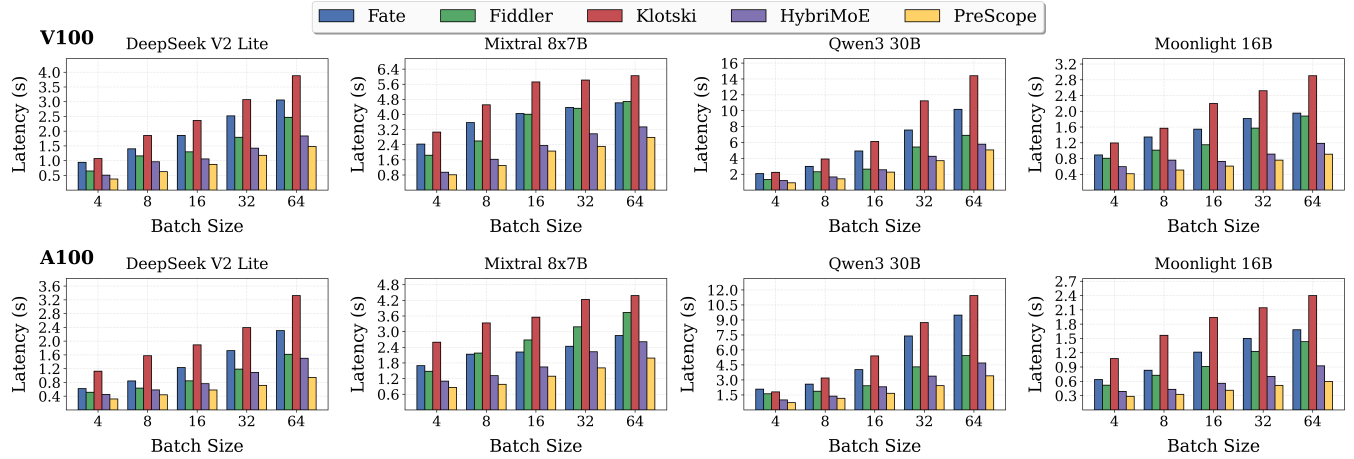


Figure 14. Decoding latency comparison between PreScope and baseline systems across models and hardware.

CPU-GPU collaborative methods, it surpasses HybriMoE by 58.7%, 37.6%, and 55.1%, and outperforms Fiddler by 71.0%, 59.6%, and 97.4%. This advantage stems from PreScope’s accurate expert prefetching mechanism and efficient scheduling optimization, which enable a higher degree of GPU-CPU parallelism. In contrast, HybriMoE, which employs a layer-by-layer scheduling strategy, shows limited performance at smaller batch sizes due to the negative I/O overhead introduced by its prefetching and dynamic expert offloading.

Large-Expert Models. The Mixtral model, with only 8 experts per layer but each occupying 336 MB, exhibits high computational intensity. As batch size increases, the CPU-GPU overhead gap widens, and PreScope’s margin over GPU-only baselines narrows. On V100, the speedup over Klotski and Fate decreases from 82.9% and 213% at batch size 8 to 14.1% and 44.3% at batch size 64. Nevertheless, PreScope maintains a clear advantage over CPU-GPU collaborative baselines: at batch size 64 on A100, it exceeds HybriMoE by 32% and Fiddler by 88%. This result indicates that in compute-intensive scenarios, expert scheduling quality directly determines the pipeline bubble ratio. Fiddler’s static hot-expert table fails to adapt to batch size variations, while HybriMoE’s greedy strategy, which prioritizes on-demand loading, contends with prefetch traffic, yielding limited gains. PreScope explicitly quantifies the trade-off between prefetch benefits and compute offload, dynamically selects CPU or GPU execution for each expert, and compresses pipeline bubbles to the theoretical minimum.

Overall, across V100/A100, four models, and batch sizes from 4 to 64, PreScope demonstrates excellent scalability, exhibiting the steepest performance growth curve in all tested scenarios. On the A100 platform, its advantage is more pronounced, particularly at larger batch sizes where precise prefetch control more efficiently leverages PCIe bandwidth enhancements for expert transfer gains. In summary, PreScope improves throughput over Fate, Fiddler, Klotski,

and HybriMoE by up to 264%, 129%, 141%, and 70.8%, respectively, scaling with PCIe bandwidth and establishing a new performance benchmark for MoE architectures.

6.2.3 Decoding Latency. Figure 14 compares the average per-token decoding latency of PreScope and four baselines on V100 and A100 GPUs. Across all batch sizes and model architectures, PreScope consistently achieves the lowest latency, owing to its precise compression of the critical path via “accurate prediction + cross-layer scheduling”.

Small-Expert Models: On V100 at batch size 4, PreScope achieves 0.37 seconds on DeepSeek, outperforming HybriMoE and Fiddler by 42.1% and 72.3%, respectively. This advantage stems from PreSched’s ability to minimize latency through cross-layer scheduling, leveraging prefetch benefits and coordinating compute/transfer more effectively than greedy strategies. At batch size 64, PreScope attains 5.05 seconds on Qwen3-30B, reducing latency by 74.6% and 46.7% compared to Klotski and Fate. While Klotski’s multi-batch pipelining improves throughput, it activates more experts simultaneously, exacerbating I/O. Fate lacks effective overhead masking and prefetch-compute parallelism, resulting in latency that scales linearly with batch size. For example, on Qwen3-30B, its latency increases by 4.6 times when the batch size increases from 4 to 64.

Large-Expert Models: Mixtral increases compute intensity, yet I/O remains the critical path bottleneck. PreScope employs a dual-pipeline “prefetch-compute” approach that hides prefetch I/O behind computation. On V100 at batch size 64, it achieves 2.79 seconds, outperforming Fate and Klotski by 30.5% and 53.9%. Klotski’s latency plateaus at 5.82 seconds for batch sizes ≥ 32 as the activated expert count reaches its limit; PreScope maintains flat latency via accurate prediction for early bandwidth release.

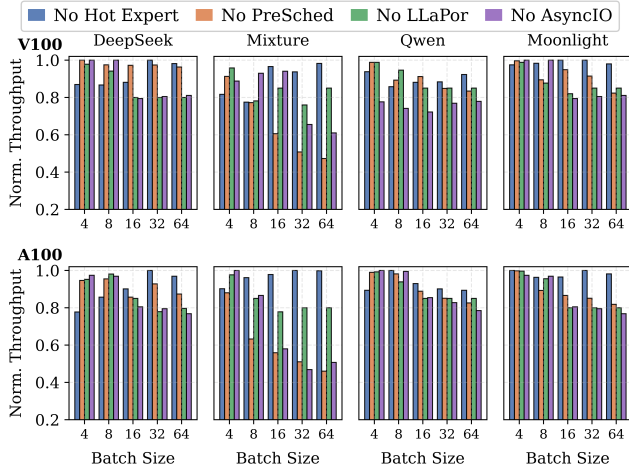


Figure 15. Throughput impact of ablating individual components in PreScope.

In summary, across architectures and batch sizes, PreScope reduces latency by up to 68.2%, 72.3%, 74.6%, and 42.1% compared to Fate, Fiddler, Klotski, and HybriMoE, demonstrating its optimization effectively adapts to both “transfer-bound” and “compute-bound” scenarios.

6.3 Ablation Study

To quantify the contribution of each module in PreScope to end-to-end throughput, we conduct a series of independent ablation studies across four MoE models, where in each run only a single component is disabled. We evaluated the impact of removing (1) the Hot Expert Table, (2) the PreSched strategy, (3) the LLaPor predictor, and (4) the AsyncIO optimizer. Comparisons are made against baselines including random preloading, fixed prefetching, layer-wise greedy loading, and native PyTorch expert loading.

The results in Figure 15 show that system bottlenecks shift with batch size. When the batch size is below 16, removing the Hot Expert Table reduces cache hit rates by 30–40%. For the DeepSeek model on V100 at batch size 4, throughput decreases by 22.2%, highlighting the critical role of the Hot Expert Table in reducing redundant transfers under light load. As the batch size exceeds 8, computational costs on the CPU rise significantly, making prefetch timing crucial. Disabling PreSched on A100 leads to a 54.1% throughput reduction for the Mixtral model at batch size 64, while removing LLaPor causes a 20.2% decrease for the Moonlight model at batch size 32. Under medium to high loads (batch size ≥ 16), disabling LLaPor or PreSched on A100 results in more severe losses, as high PCIe bandwidth allows more prefetch operations to be scheduled during CPU computation, increasing the prefetch ratio. Disabling AsyncIO serializes expert transfers and computations, and Pytorch’s coarse-grained operations are over 70% slower than AsyncIO’s fine-grained approach,

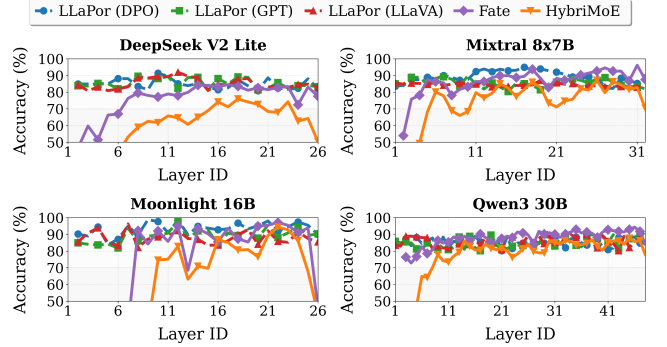


Figure 16. Prediction accuracy of LLaPor across different models and datasets.

Table 3. Performance Evaluation of LLaPor.

	DeepSeek	Mixtral	Qwen3	Moonlight
Top2	100%	100%	100%	100%
Top3	97%	100%	99%	100%
Top4	94%	99%	97%	99%
Tokens	95%	97%	97%	98%
Memory	0.6-2.7 MB	0.5-2.5 MB	0.5-2.8 MB	0.6-2.7 MB
Time	0.48 ms	0.15 ms	0.12 ms	0.48 ms

leading to a sharp drop in PCIe utilization. This impact is particularly pronounced under medium to high loads; for example, throughput decreases by 49.3% for Mixtral on A100 at batch size 64.

In summary, the Hot Expert Table ensures cache efficiency under light load; PreSched and AsyncIO jointly optimize compute-I/O overlap at medium/high loads via scheduling and execution improvements; and LLaPor provides reliable future expert activation visibility. All four components are indispensable—removing any results in 20–54% performance degradation, validating the necessity and robustness of PreScope’s design.

6.4 Predictor Accuracy

To evaluate the generalization capability and prediction accuracy of LLaPor, we conduct tests across four MoE models and three public datasets (ShareGPT, DPO, LLaVA). The evaluation uses a batch size of 32, with 128 input tokens and 32 output tokens. We compare the Top-k experts selected by the gating network with those predicted by LLaPor and compute the hit rate. As shown in Figure 16, LLaPor performs consistently across all models, achieving the highest accuracy on Moonlight and the lowest on DeepSeek, yet never drops below 80% for any model or layer. These results align with Section 3.2: accuracy positively correlates with the cosine similarity of hidden states between adjacent layers and inter-layer expert correlations. Even in input and output layer groups with low similarity, LLaPor confines prediction errors within the Top-6, preventing prefetch inaccuracies

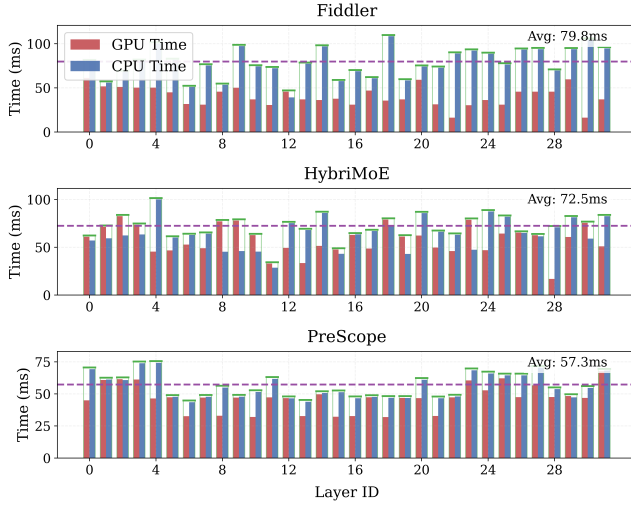


Figure 17. Per-layer time breakdown comparison between PreScope and collaborative inference baseline methods.

from affecting subsequent scheduling. Compared to state-of-the-art gate-based prediction methods, LLaPor improves accuracy by 15%–68.4%.

We further examine the impact of LLaPor on end-to-end operation. Table 3 shows the "hot Top-4" prefetch accuracy: experts are ranked by token volume, and with a second-order sliding window (i.e., a prediction is considered correct if the Top-4 falls within the true Top-6), LLaPor achieves a Top-4 hit rate of no less than 94%, corresponding to a token coverage error below 5%, meeting PreSched’s precision requirement for CPU-side overhead estimation. For resource usage, each model deploys one micro-predictor per layer, with per-predictor parameters as low as 0.5 MB. Middle-layer predictors have slightly deeper structures, with a maximum footprint of 2.8 MB per layer. Initial training takes 30 epochs, each requiring 0.6 seconds on A100. Periodic fine-tuning costs are much lower than initial training, as it uses few samples collected during inference and requires only limited iterations, with latency controllable within milliseconds. During inference, single forward-pass latency remains stable between 0.12–0.48 ms, which can be fully hidden within gaps where the GPU awaits expert transfers, introducing no additional bubbles. These results demonstrate that LLaPor satisfies "high hit rate, low resource consumption, and zero inference overhead" simultaneously, providing a reliable and lightweight prior for PreScope’s cross-layer scheduling.

6.5 CPU-GPU Parallelism

The key to CPU-GPU collaborative inference lies in maximizing parallelism between the CPU and GPU. Figure 17 shows the cumulative distribution of per-layer CPU and GPU thread overheads for Mixtral on A100. PreScope confines the gap between the two within 8 ms for 50% of the layers;

the remaining layers exhibit a peak difference of about 14 ms, aligning exactly with the latency of one expert prefetch. This indicates that LLaPor and PreSched, through a "two-layer lookahead" mechanism, decouple prefetch overhead from the critical path, achieving precise overlap of CPU computation with GPU computation and transfer. Furthermore, PreScope prevents high CPU thread overhead in layers containing numerous hot experts (mostly non-resident in GPU during initialization)—PreSched’s cross-layer scheduling anticipates such scenarios and reserves on-demand loading opportunities in previous layers for prefetching larger experts, thereby balancing the load. In contrast, HybriMoE does not account for prefetch effects when placing experts, often prefetching too many experts in the current layer and delaying on-demand loading for the next layer, resulting in higher GPU than CPU thread overhead (e.g., layers 9–10). Alternatively, it fails to leverage CPU-GPU overhead differences for sufficient prefetching or suffers prefetch failures, leaving the next layer’s overhead unoptimized (e.g., layers 28–29). Fiddler, lacking the cold-hot expert queue, retains 70% of hot experts on the CPU, causing average CPU thread overhead to be 1.9 times that of the GPU and yielding the lowest parallelism. Experiments show that PreScope, via prediction-driven cross-layer scheduling, compresses the CPU-GPU thread overhead difference to within a single prefetch granularity, significantly outperforming static or greedy strategies and providing a quantifiable upper bound for collaborative inference parallelism.

7 Conclusion

This work presents PreScope to address the memory bottleneck and PCIe latency in MoE inference under resource-constrained environments. By jointly modeling the current layer and the prefetch-target layer, PreScope reformulates expert on-demand loading and prefetching decisions into a global latency-aware expert placement optimization problem. Three co-designed core components collectively address the associated challenges: LLaPor ensures accurate target-layer information through group-aware prediction; PreSched constructs a pipeline model incorporating I/O, GPU, and CPU execution within the cross-layer framework, and searches for latency-optimal scheduling strategies; AsyncIO provides system-level support to achieve full overlap between I/O operations and GPU computation while maximizing PCIe bandwidth utilization efficiency. Evaluations on four MoE models show that PreScope improves throughput by 141% and reduces decoding latency by 74.6% compared to state-of-the-art baselines, while maintaining stable scalability from batch size 4 to 64 on both V100 and A100 GPUs. Future work will generalize the PreScope cost model to multi-GPU domains, incorporate low-precision expert compression, and explore co-design with emerging memory hierarchies.

References

- [1] Anonymous. 2024. ShareGPT-V3-unfiltered-cleaned-split. Electronic dataset. https://huggingface.co/datasets/learnanything/sharegpt_v3_unfiltered_cleaned_split
- [2] Jason Ansel, Edward Yang, Horace He, Natalia Gimelshein, Animesh Jain, Michael Voznesensky, Bin Bao, Peter Bell, David Berard, Evgeni Burovski, et al. 2024. Pytorch 2: Faster machine learning through dynamic python bytecode transformation and graph compilation. In *ACM ASPLOS*. 929–947.
- [3] Shiyi Cao, Shu Liu, Tyler Griggs, Peter Schafhalter, Xiaoxuan Liu, Ying Sheng, Joseph E Gonzalez, Matei Zaharia, and Ion Stoica. 2025. Moe-lightning: High-throughput moe inference on memory-constrained gpus. In *ACM ASPLOS*. 715–730.
- [4] Hongtao Chen, Weiyu Xie, Boxin Zhang, Jingqi Tang, Jiahao Wang, Jianwei Dong, Shaoyuan Chen, Ziwei Yuan, Chen Lin, Chengyu Qiu, Yuening Zhu, Qingliang Ou, Jiaqi Liao, Xianglin Chen, Zhiyuan Ai, Yongwei Wu, and Mingxing Zhang. 2025. KTransformers: Unleashing the Full Potential of CPU/GPU Hybrid Inference for MoE Models. In *ACM SOSP*. 10–26.
- [5] Le Chen, Dahu Feng, Erhu Feng, Rong Zhao, Yingrui Wang, Yubin Xia, Haibo Chen, and Pinjie Xu. 2025. HeteroLLM: Accelerating Large Language Model Inference on Mobile SoCs platform with Heterogeneous AI Accelerators. arXiv:2501.14794
- [6] Peizhuang Cong, Aomufei Yuan, Shimao Chen, Yuxuan Tian, Bowen Ye, and Tong Yang. 2024. Prediction is all moe needs: Expert load distribution goes from fluctuating to stabilizing. arXiv:2404.16914
- [7] Hongchao Du, Shangyu Wu, Arina Kharlamova, Nan Guan, and Chun Jason Xue. 2025. FlexInfer: Breaking Memory Constraint via Flexible and Efficient Offloading for On-Device LLM Inference. In *EuroMLSys*. 56–65.
- [8] Zhixu Du, Shiyu Li, Yuhao Wu, Xiangyu Jiang, Jingwei Sun, Qilin Zheng, Yongkai Wu, Ang Li, Hai Li, and Yiran Chen. 2024. Sida: Sparsity-inspired data-aware serving for efficient and scalable large mixture-of-experts models. *MLSys* 6 (2024), 224–238.
- [9] Haojie Duanmu, Xiuhong Li, Zhihang Yuan, Size Zheng, Jiangfei Duan, Xingcheng Zhang, and Dahua Lin. 2025. MxMoE: Mixed-precision Quantization for MoE with Accuracy and Performance Co-Design. arXiv:2505.05799
- [10] Zhiyuan Fang, Zicong Hong, Yuegui Huang, et al. 2025. Fate: Fast Edge Inference of Mixture-of-Experts Models via Cross-Layer Gate. arXiv:2502.12224
- [11] Zhiyuan Fang, Yuegui Huang, Zicong Hong, Yufeng Lyu, Wuhui Chen, Yue Yu, Fan Yu, and Zibin Zheng. 2025. Klotski: Efficient Mixture-of-Expert Inference via Expert-Aware Multi-Batch Pipeline. In *ACM ASPLOS*. 574–588.
- [12] William Fedus, Barret Zoph, and Noam Shazeer. 2022. Switch transformers: Scaling to trillion parameter models with simple and efficient sparsity. *JMLR* 23, 120 (2022), 1–39.
- [13] Elias Frantar and Dan Alistarh. 2023. Qmoe: Practical sub-1-bit compression of trillion-parameter models. arXiv:2310.16795
- [14] Yongxin Guo, Zhenglin Cheng, Xiaoying Tang, Zhaopeng Tu, and Tao Lin. 2024. Dynamic mixture of experts: An auto-tuning approach for efficient transformer models. arXiv:2405.14297
- [15] Vima Gupta, Kartik Sinha, Ada Gavrilovska, and Anand Padmanabha Iyer. 2024. Lynx: Enabling Efficient MoE Inference through Dynamic Batch-Aware Expert Selection. arXiv:2411.08982
- [16] Xin He, Shunkang Zhang, Yuxin Wang, Haiyan Yin, Zihao Zeng, Shaohuai Shi, Zhenheng Tang, Xiaowen Chu, Ivor Tsang, and Ong Yew Soon. 2024. Expertflow: Optimized expert activation and token allocation for efficient mixture-of-experts inference. arXiv:2410.17954
- [17] Huanqi Hu, Bowen Xiao, Shixuan Sun, Jianian Yin, Zhexi Zhang, Xiang Luo, Chengquan Jiang, Weiqi Xu, Xiaoying Jia, Xin Liu, et al. 2025. LiquidGEMM: Hardware-Efficient W4A8 GEMM Kernel for High-Performance LLM Serving. arXiv:2509.01229
- [18] Haiyang Huang, Newsha Ardalani, Anna Sun, Liu Ke, Shruti Bhosale, Hsien-Hsin Lee, Carole-Jean Wu, and Benjamin Lee. 2024. Toward efficient inference for mixture of experts. *NIPS* 37 (2024), 84033–84059.
- [19] Rangi Hwang, Jianyu Wei, Shijie Cao, Changho Hwang, Xiaohu Tang, Ting Cao, and Mao Yang. 2024. Pre-gated moe: An algorithm-system co-design for fast and scalable mixture-of-expert inference. In *IEEE ISCA*. 1018–1031.
- [20] Albert Q Jiang, Alexandre Sablayrolles, Antoine Roux, Arthur Mensch, Blanche Savary, Chris Bamford, Devendra Singh Chaplot, Diego de las Casas, Emma Bou Hanna, Florian Bressand, et al. 2024. Mixtral of experts. arXiv:2401.04088
- [21] Zewen Jin, Shengnan Wang, Jiaan Zhu, Hongrui Zhan, Youhui Bai, Lin Zhang, Zhenyu Ming, and Cheng Li. 2025. BigMac: A Communication-Efficient Mixture-of-Experts Model Structure for Fast Training and Inference. In *AAAI*. 17689–17698.
- [22] Keisuke Kamahori, Tian Tang, Yile Gu, Kan Zhu, and Baris Kasikci. 2025. Fiddler: CPU-GPU Orchestration for Fast Inference of Mixture-of-Experts Models. In *ICLR*. 56099–56115.
- [23] Woosuk Kwon, Zhuohan Li, Siyuan Zhuang, Ying Sheng, Lianmin Zheng, Cody Hao Yu, Joseph Gonzalez, Hao Zhang, and Ion Stoica. 2023. Efficient memory management for large language model serving with pagedattention. In *ACM SOSP*. 611–626.
- [24] Xinlu Lai. 2024. The DPO Dataset for Chinese and English with emoji. <https://huggingface.co/datasets/shareAI/DPO-zh-en-emoji>.
- [25] Wonbeom Lee, Jungi Lee, Junghwan Seo, and Jaewoong Sim. 2024. InfiniGen: Efficient generative inference of large language models with dynamic {KV} cache management. In *OSDI*. 155–172.
- [26] Jiamin Li, Yimin Jiang, Yibo Zhu, Cong Wang, and Hong Xu. 2023. Accelerating distributed MoE training and inference with lina. In *USENIX ATC* 23. 945–959.
- [27] Aixin Liu, Bei Feng, Bin Wang, Bingxuan Wang, Bo Liu, Chenggang Zhao, Chengqi Deng, Chong Ruan, Damai Dai, Daya Guo, et al. 2024. Deepseek-v2: A strong, economical, and efficient mixture-of-experts language model. arXiv:2405.04434
- [28] Haotian Liu, Chunyuan Li, Qingyang Wu, and Yong Jae Lee. 2023. Visual instruction tuning. *NIPS* 36 (2023), 34892–34916.
- [29] Jingyuan Liu, Jianlin Su, Xingcheng Yao, Zhejun Jiang, Guokun Lai, Yulun Du, Yidao Qin, et al. 2025. Muon is Scalable for LLM Training. arXiv:2502.16982
- [30] Xudong Lu, Qi Liu, Yuhui Xu, Aojun Zhou, Siyuan Huang, Bo Zhang, Junchi Yan, and Hongsheng Li. 2024. Not all experts are equal: Efficient expert pruning and skipping for mixture-of-experts large language models. arXiv:2402.14800
- [31] Zhiwen Mo, Lei Wang, Jianyu Wei, Zhichen Zeng, Shijie Cao, Lingxiao Ma, Naifeng Jing, Ting Cao, Jilong Xue, Fan Yang, et al. 2025. LUT Tensor Core: A Software-Hardware Co-Design for LUT-Based Low-Bit LLM Inference. In *ISCA*. 514–528.
- [32] OpenAI, Josh Achiam, Steven Adler, Sandhini Agarwal, Lama Ahmad, Ilge Akkaya, Florencia Leoni Aleman, et al. 2024. GPT-4 Technical Report. arXiv:2303.08774
- [33] Xiurui Pan, Endian Li, Qiao Li, Shengwen Liang, Yizhou Shan, Ke Zhou, Yingwei Luo, Xiaolin Wang, and Jie Zhang. 2025. InstAttention: In-Storage Attention Offloading for Cost-Effective Long-Context LLM Inference. In *IEEE HPCA*. 1510–1525.
- [34] Samyam Rajbhandari, Conglong Li, Zhewei Yao, Minjia Zhang, Reza Yazdani Aminabadi, Ammar Ahmad Awan, Jeff Rasley, and Yuxiong He. 2022. DeepSpeed-moe: Advancing mixture-of-experts inference and training to power next-generation ai scale. In *ICML*. 18332–18346.
- [35] Samyam Rajbhandari, Olatunji Ruwase, Jeff Rasley, Shaden Smith, and Yuxiong He. 2021. Zero-infinity: Breaking the gpu memory wall for extreme scale deep learning. In *ACM SC*. 1–14.
- [36] Jay Shah, Ganesh Bikshandi, Ying Zhang, Vijay Thakkar, Pradeep Ramani, and Tri Dao. 2024. Flashattention-3: Fast and accurate attention

- with asynchrony and low-precision. *NIPS* 37 (2024), 68658–68685.
- [37] Ying Sheng, Lianmin Zheng, Binhang Yuan, Zhuohan Li, Max Ryabinin, Beidi Chen, Percy Liang, Christopher Ré, Ion Stoica, and Ce Zhang. 2023. Flexgen: High-throughput generative inference of large language models with a single gpu. In *ICML*. 31094–31116.
- [38] Xiaoni Song, Zihang Zhong, Rong Chen, and Haibo Chen. 2024. Promoe: Fast moe-based llm serving using proactive caching. arXiv:2410.22134
- [39] Yixin Song, Zeyu Mi, Haotong Xie, and Haibo Chen. 2024. PowerInfer: Fast Large Language Model Serving with a Consumer-grade GPU. In *ACM SOSR*. 590–606.
- [40] Ruslan Svirschevski, Avner May, Zhuoming Chen, Beidi Chen, Zhihao Jia, and Max Ryabinin. 2024. Specexec: Massively parallel speculative decoding for interactive llm inference on consumer devices. *NIPS* 37 (2024), 16342–16368.
- [41] Peng Tang, Jiacheng Liu, Xiaofeng Hou, Yifei Pu, Jing Wang, Pheng-Ann Heng, Chao Li, and Minyi Guo. 2024. Hobbit: A mixed precision expert offloading system for fast moe inference. arXiv:2411.01433
- [42] Wei Tao, Haocheng Lu, Xiaoyang Qu, Bin Zhang, Kai Lu, Jiguang Wan, and Jianzong Wang. 2025. MoQAE: Mixed-Precision Quantization for Long-Context LLM Inference via Mixture of Quantization-Aware Experts. arXiv:2506.07533
- [43] Qwen Team. 2025. Qwen3 Technical Report. arXiv:2505.09388 [cs.CL] <https://arxiv.org/abs/2505.09388>
- [44] Yiding Wang, Kai Chen, Haisheng Tan, and Kun Guo. 2023. Tabi: An efficient multi-level inference system for large language models. In *EuroSys*. 233–248.
- [45] Yuanxin Wei, Jianguo Du, Jiazhi Jiang, Xiao Shi, Xianwei Zhang, Dan Huang, Nong Xiao, and Yutong Lu. 2024. APTMoE: Affinity-Aware Pipeline Tuning for MoE Models on Bandwidth-Constrained GPU Nodes. In *IEEE SC*. 1–14.
- [46] Thomas Wolf, Lysandre Debut, Victor Sanh, Julien Chaumond, Clement Delangue, Anthony Moi, Pierric Cistac, Tim Rault, Rémi Louf, Morgan Funtowicz, et al. 2019. Huggingface’s transformers: State-of-the-art natural language processing. arXiv:1910.03771
- [47] Daliang Xu, Wangsong Yin, Hao Zhang, Xin Jin, Ying Zhang, Shiyun Wei, Mengwei Xu, and Xuanzhe Liu. 2025. EdgeLLM: Fast On-Device LLM Inference With Speculative Decoding. *IEEE TMC* 24, 4 (2025), 3256–3273.
- [48] Tairan Xu, Leyang Xue, Zhan Lu, Adrian Jackson, and Luo Mai. 2025. MoE-Gen: High-Throughput MoE Inference on a Single GPU with Module-Based Batching. arXiv:2503.09716
- [49] Fuzhao Xue, Zian Zheng, Yao Fu, Jinjie Ni, Zangwei Zheng, Wangchunshu Zhou, and Yang You. 2024. OpenMoE: an early effort on open mixture-of-experts language models. In *ICML*. 55625–55655.
- [50] Leyang Xue, Yao Fu, Zhan Lu, Luo Mai, and Mahesh Marina. 2025. MoE-Infinity: Efficient MoE Inference on Personal Machines with Sparsity-Aware Expert Cache. arXiv:2401.14361
- [51] Jinghan Yao, Quentin Anthony, Aamir Shafi, Hari Subramoni, and Dhabaleswar K DK Panda. 2024. Exploiting inter-layer expert affinity for accelerating mixture-of-experts model inference. In *IEEE IPDPS*. 915–925.
- [52] Hanfei Yu, Xingqi Cui, Hong Zhang, and Hao Wang. 2025. fMoE: Fine-Grained Expert Offloading for Large Mixture-of-Experts Serving. arXiv:2502.05370
- [53] Libo Zhang, Zhaoning Zhang, Baizhou Xu, Songzhu Mei, and Dongsheng Li. 2025. Dovetail: A cpu/gpu heterogeneous speculative decoding for llm inference. In *EMNLP*. 1–13.
- [54] Yujie Zhang, Shivam Aggarwal, and Tulika Mitra. 2025. DAOP: Data-Aware Offloading and Predictive Pre-Calculation for Efficient MoE Inference. In *IEEE DATE*. 1–7.
- [55] Xuanlei Zhao, Bin Jia, Haotian Zhou, Ziming Liu, Shenggan Cheng, and Yang You. 2024. Hetegen: Efficient heterogeneous parallel inference for large language models on resource-constrained devices. *MLSys* 6 (2024), 162–172.
- [56] Shuzhang Zhong, Ling Liang, Yuan Wang, Runsheng Wang, Ru Huang, and Meng Li. 2024. AdapMoE: Adaptive sensitivity-based expert gating and management for efficient moe inference. In *IEEE ICCAD*. 1–9.
- [57] Shuzhang Zhong, Yanfan Sun, Ling Liang, Runsheng Wang, Ru Huang, and Meng Li. 2025. HybriMoE: Hybrid CPU-GPU Scheduling and Cache Management for Efficient MoE Inference. In *DAC*. 1–7.